

High-Resolution Vibrational Spectra of Furazan

I. The B_1 Fundamental ν_{12} and the A_1 Fundamental ν_5 from Fourier-Transform Infrared Spectroscopy

Otto L. Stiefvater

Coleg Prifysgol Gogledd Cymru, Bangor LL57 2UW, Wales, U.K.

Z. Naturforsch. **46a**, 841–850 (1991); received July 17, 1991

The study by Fourier transform (FT) infrared (IR) spectroscopy of the fundamental vibrational bands ν_{12} and ν_5 of furazan yields the origins of these bands with a statistical uncertainty of 10^{-6} cm^{-1} , which leads to an estimated absolute uncertainty of 10^{-4} cm^{-1} . The values are $\nu_{12}^0 = 952.6123 \text{ cm}^{-1}$ and $\nu_5^0 = 1.005.3536 \text{ cm}^{-1}$. They confirm the values previously deduced from laser/microwave double resonance (LMDR) experiments.

Previous results for the molecular constants of the vibrational ground state and of the two vibrationally excited states, as obtained by double resonance modulation (DRM) microwave spectroscopy alone, are confirmed and refined.

Advantages brought about through the combination of the DRM microwave and the FT-IR technique are outlined.

I. Introduction

Almost concurrently with our efforts to determine the vibrational band origins for the modes ν_{12} and ν_5 of furazan ($\text{C}_2\text{H}_2\text{N}_2\text{O}$) through laser/microwave double resonance (LMDR) experiments [1], the introduction of interferometric principles (with subsequent Fourier transformation (FT) of the interferogram) into vibrational spectroscopy began to raise the spectral resolution of commercially available infrared (IR) spectrometers. With almost breath-taking speed this process reached its natural limitation in the Doppler width of vibrational transitions by the end of the 1980s.

This much appreciated instrumental development made a renewed examination of the vibrational spectrum of furazan – now by FT-IR spectroscopy and over the entire wavenumber range of fundamentals – desirable. Such work was carried out in the laboratory of Prof. M. Winnewisser at the University Giessen (FRG). Hence, we are now in possession of the entire high-resolution IR-spectrum of furazan, recorded on the commercial FT-IR instrument (Bruker IFS 120 HR) at Giessen during the summer of 1990. As was expected, this experimental information is complementary to the molecular information previously established by DRM microwave work [2] and then augmented by the LMDR experiments [1].

Reprint requests to Dr. O. L. Stiefvater, Coleg Prifysgol Gogledd Cymru, Bangor LL57 2UW, Wales, U.K.

While the successive analysis of all IR-detectable vibrational bands of furazan against the background of rotational information on the same bands is in progress, it seems appropriate to communicate, as a first installment of that work, the results obtained for the bands ν_{12} and ν_5 from high-resolution FT-IR spectrometry.

II. Experimental, Theory and Computational

The fundamentals ν_{12} and ν_5 were recorded twice on the Bruker IFS 120 HR FT-interferometer. In the first experiment a conventional 'short' sample cell (path length 28 cm, KBr windows) was used containing furazan vapour at a pressure of $\sim 5 \text{ mbar}$ (500 pa) at room temperature. After a 'long' sample cell of path length 300 cm had become available and had been installed, the furazan bands were re-recorded at the lower pressure of $\sim 0.5 \text{ mbar}$. The recordings were taken with a Globar as the source of radiation, and a Ge–Cu crystal at liquid helium temperature (4.2 K) was used as detector. The interferogram was built up from 60 coadded scans in the case of ν_5 and from 180 scans in the case of ν_{12} . The spectral resolution was 0.0028 cm^{-1} and 0.0022 cm^{-1} , respectively. Both spectra were calibrated against N_2O lines [3], recorded immediately after the sample runs.

The numerical analysis of the spectral data was carried out with the help of a computer program writ-

0932-0784 / 91 / 1000-0841 \$ 01.30/0. – Please order a reprint rather than making your own copy.



Dieses Werk wurde im Jahr 2013 vom Verlag Zeitschrift für Naturforschung in Zusammenarbeit mit der Max-Planck-Gesellschaft zur Förderung der Wissenschaften e.V. digitalisiert und unter folgender Lizenz veröffentlicht: Creative Commons Namensnennung-Keine Bearbeitung 3.0 Deutschland Lizenz.

Zum 01.01.2015 ist eine Anpassung der Lizenzbedingungen (Entfall der Creative Commons Lizenzbedingung „Keine Bearbeitung“) beabsichtigt, um eine Nachnutzung auch im Rahmen zukünftiger wissenschaftlicher Nutzungsformen zu ermöglichen.

This work has been digitalized and published in 2013 by Verlag Zeitschrift für Naturforschung in cooperation with the Max Planck Society for the Advancement of Science under a Creative Commons Attribution-NoDerivs 3.0 Germany License.

On 01.01.2015 it is planned to change the License Conditions (the removal of the Creative Commons License condition "no derivative works"). This is to allow reuse in the area of future scientific usage.

ten by Gambi [4] during his stay at Giessen. At the heart of this routine lies the assumption (condition) that the vibrationally connected rotational energy manifolds are free from effects arising from other vibrational modes (Coriolis interactions) and that they can therefore be adequately described by Watson's [5] A-reduced Hamiltonian:

$$\begin{aligned}\hat{H}_{\text{rot}} = & \frac{1}{2}(B+C)\hat{P}^2 \\ & + (A - \frac{1}{2}(B+C))\hat{P}_a^2 - \Delta_J\hat{P}^4 - \Delta_{JK}\hat{P}^2\hat{P}_a^2 - \Delta_K\hat{P}_a^4 \\ & + \Phi_J\hat{P}^6 + \Phi_{JK}\hat{P}^4\hat{P}_a^2 + \Phi_{KJ}\hat{P}^2\hat{P}_a^4 + \Phi_K\hat{P}_a^6 \\ & + (\frac{1}{2}(B-C) - 2\delta_J\hat{P}^2 + 2\varphi_J\hat{P}^4) \cdot (\hat{P}_b^2 - \hat{P}_c^2) \\ & + [(-\delta_K\hat{P}_a^2 + \varphi_{JK}\hat{P}^2\hat{P}_a^2 + \varphi_K\hat{P}_a^4), (\hat{P}_b^2 - \hat{P}_c^2)]_+.\end{aligned}\quad (1)$$

In this expression, A , B , and C are the reduced rotational constants and \hat{P} is the angular momentum operator with components \hat{P}_a , \hat{P}_b , and \hat{P}_c along the inertial axes, a , b , c . The greek delta (Δ , δ) represents the quartic distortion constants, while the sextic distortion constants are indicated by the symbols Φ and φ . The third line in (1) is the product between the bracketed operator combinations and the last line denotes the anti-commutator, $[\cdot, \cdot]_+$, between the bracketed combinations. – When the above assumption is met, the wavenumber values ν_i of the rovibrational transitions of an IR absorption band from a lower to a higher vibrational state are given as

$$\begin{aligned}\nu_i(\Delta J, \Delta K_a, \Delta K_c, \nu^0) \\ = \nu^0 + E_{h, \text{rot}}(J', K'_a, K'_c) - E_{l, \text{rot}}(J, K_a, K_c),\end{aligned}\quad (2)$$

where ν^0 is the band origin and $E_{h, \text{rot}}$ are the eigenvalues of the Hamiltonian (1) for the higher vibrational level, with a corresponding meaning of $E_{l, \text{rot}}$ for the lower level. ΔJ , ΔK_a , and ΔK_c are the changes in the rotational quantum numbers involved in a rovibrational transition. They are given by the well-known dipole selection rules.

The computer package by A. Gambi consists of two parts, of which the first one (TRANSI) permits the computation of an IR band-structure from known (or assumed) rotational parameters for the ground state (G.S.) and for the vibrationally excited state in question, together with the known (or assumed) wavenumber ν^0 of the band origin. There are thus 31 parameters (ν^0 and 15 constants for each state (3 rotational constants, 5 quartic and 7 sextic distortion constants)) to be specified for a band. The other part of the computer routine is a least-squares (LSQ) fitting procedure (MINIQ) for the extraction of these molecular con-

stants from a set of identified (assigned) rovibrational transitions of a measured band. A feature of MINIQ which we found particularly useful in our application lies in the fact that MINIQ permits the inclusion in the LSQ-fit of pure rotational transitions within the G.S. and/or within the vibrationally excited state.

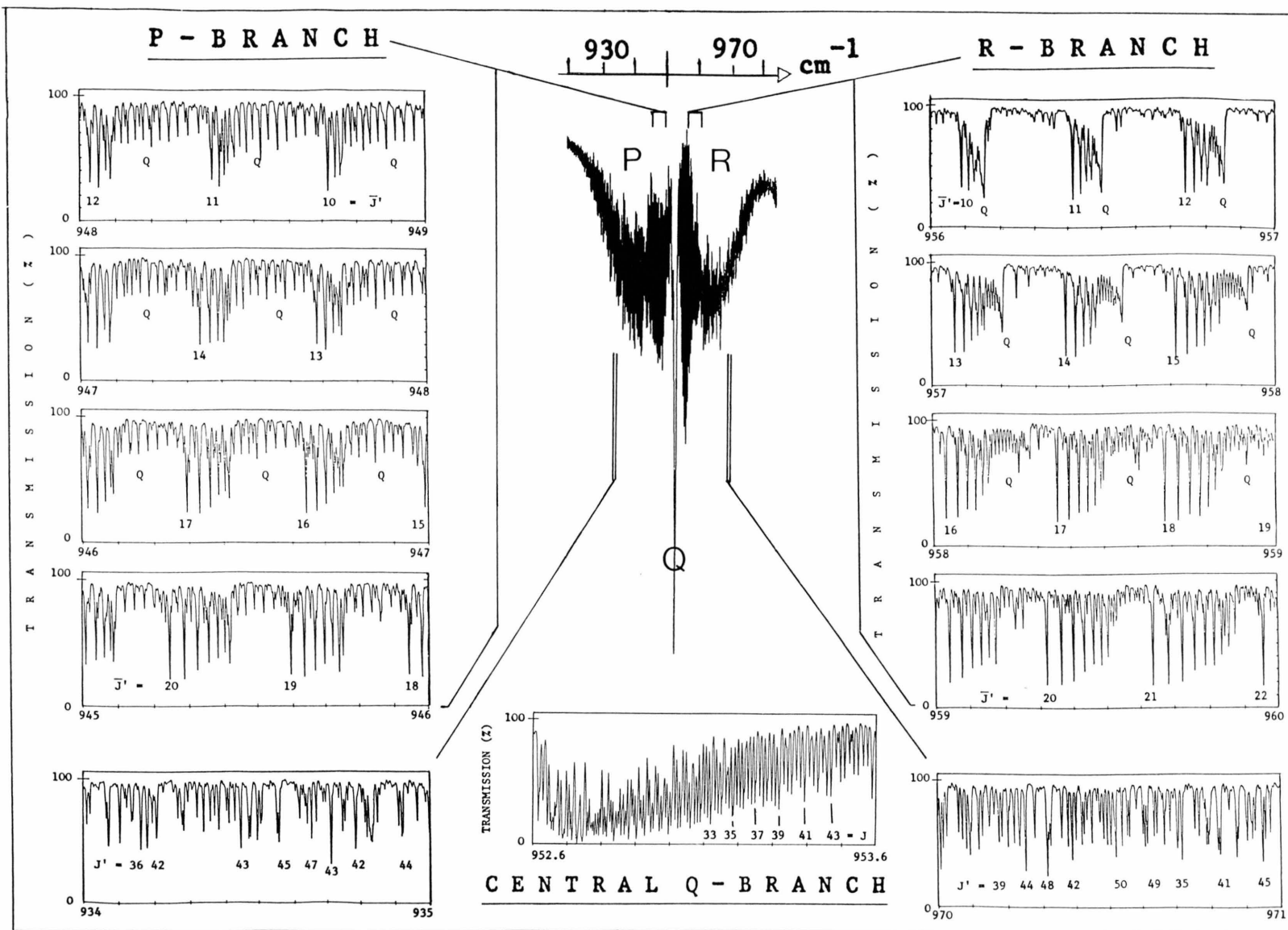
III. Results

1. Assignments within the Bands ν_{12} and ν_5

As a results of the comprehensive background information, – consisting of the vibrational origins ν_{12}^0 and ν_5^0 as determined in the earlier LMDR experiments [1], and of the rotational constants for the G.S. as well as for the two excited states as previously determined from DRM microwave work [2] –, which was available for insertion into the TRANSI program, the correlation of observed IR transitions of the two fundamentals with rotational quantum numbers J , K_a , K_c of the levels of the G.S. and J' , K'_a , K'_c of the levels in the excited state offered no difficulty. Under restriction to ranges of $\sim 25 \text{ cm}^{-1}$ on either side of the band origins it was readily possible to assign some 3300 rovibrational transitions of the ν_{12} -band and some 2400 lines within the ν_5 -band. In each case the mentioned wavenumber ranges contain the majority of transitions with J -values up to 50. For both bands the numbers of P-, Q- and R-branch lines is roughly comparabile (see Table 2 for actual numbers).

2. Qualitative description of the two IR-Bands

The band structures of ν_{12} and ν_5 are shown in Figs. 1 and 2. The overall, compressed band contour is shown in the middle of these figures and selected portions of each band are arranged at full resolution around the outside. Tables of the observed peak wavenumbers for both bands have been deposited with the 'Sektion für Spektren und Strukturdokumentation' of the Universität Ulm, Postfach 40 66, D-7900 Ulm. These lists may also be obtained from the author. In both figures some values of J' have been inserted for correlation with the following descriptions of the bands. J -values for individual Q-branch transitions have been omitted though for the sake of clarity of the traces. Unabbreviated asymmetric rotor notation is used for the description of transitions.

Fig. 1. The A-type band ν_{12} at $\sim 953 \text{ cm}^{-1}$ with high-resolution sections.

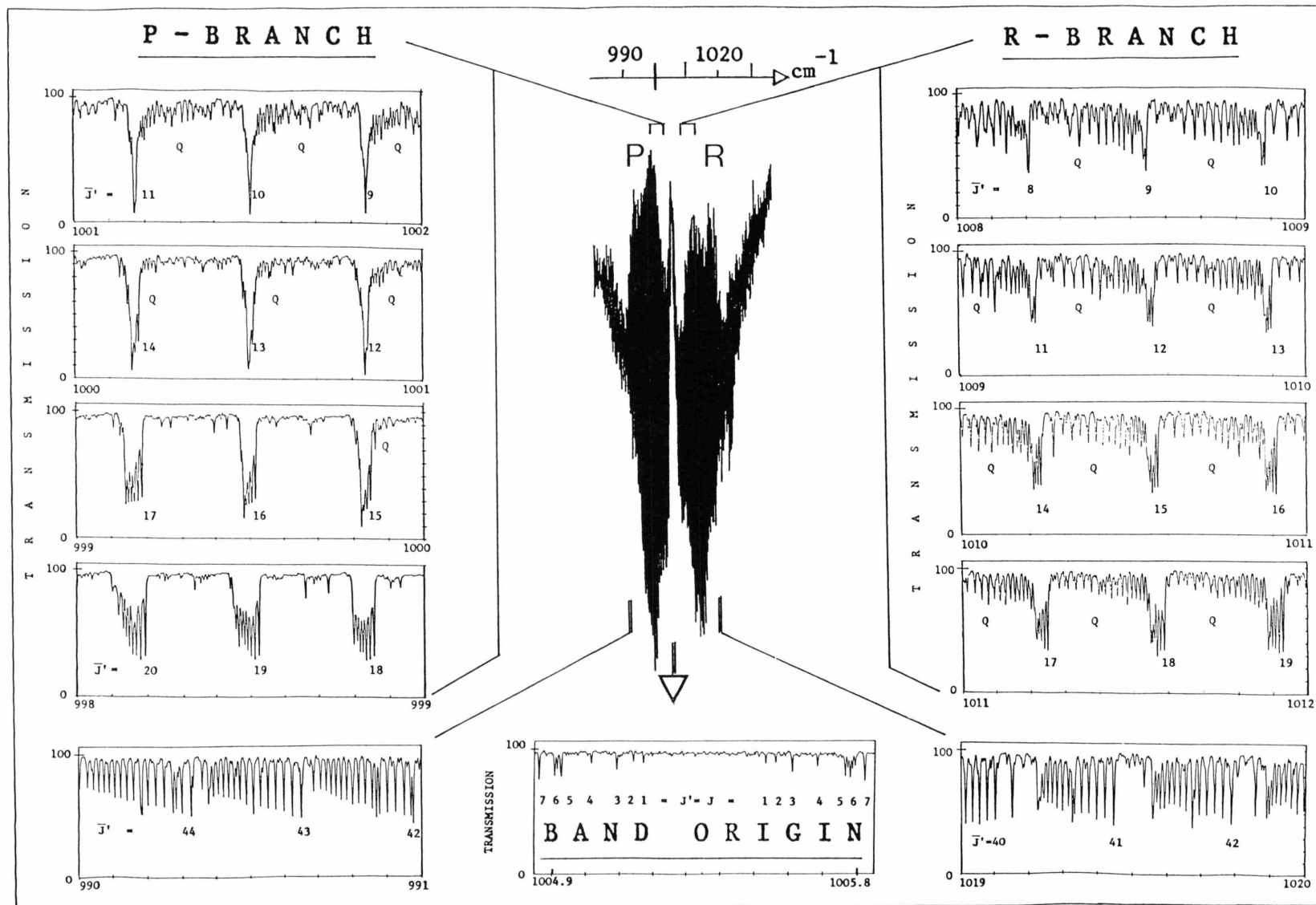


Fig. 2. The B-type band ν_s at $\sim 1005 \text{ cm}^{-1}$ with high-resolution sections.

The A-type Band ν_{12}

As generally expected, quantitatively pre-calculated (TRANSI) and experimentally observed (Fig. 1), the P- and R-branch sides of this band consist of clusters of transitions of the doubly degenerate type

$$\begin{aligned}\bar{J}'_{[0/1], \bar{J}'} &\leftarrow J^*_{[0/1], J^*}, \\ (\bar{J}' - 1)_{[1/2], (\bar{J}' - 2)} &\leftarrow (J^* - 1)_{[1/2], (J^* - 2)}, \\ (\bar{J}' - 2)_{[2/3], (J' - 4)} &\leftarrow (J^* - 2)_{[2/3], (J^* - 4)}, \text{ etc.,}\end{aligned}$$

where $J^* = \bar{J}' - 1$ for the R-branch side and $J^* = \bar{J}' + 1$ for the P-branch side. \bar{J}' is the leading (highest) principal quantum number for each such $|\Delta J| = 1$ cluster and inserted in Figure 1. The degeneracy is indicated by the square brackets which contain the two degenerate K_a -values. (Furazan is an oblate molecule with $\kappa = +0.714527$.) Within each such cluster the wavenumbers of transitions increase with decreasing J' . While for low values of \bar{J}' the clusters comprise few members and are separated from each other, they contain more and more transitions as \bar{J}' increases, thereby gradually filling the gap between successive clusters. Eventually, at $\bar{J}' \sim 25$ successive clusters flow into each other with the result that the weakest transitions (lowest values of J') with the highest wavenumbers of one cluster become overlapped by the strong high J' members at the start of the next cluster. At very high J' -values this readily discernable structure of the band is lost (see bottom right and left hand traces in Figure 1).

The gaps between successive $|\Delta J| = 1$ groups of transitions in the low and intermediate \bar{J}' -range ($\bar{J}' < 20$) provide space for the observation of Q-branch transitions or series of such transitions which are of smaller intensity. These are of the K_a -degenerate type

$$J'_{[(J' - n)/(J' - n + 1)], n} \leftarrow J_{[(J - n)/(J - n - 1)], (n + 1)}$$

on the upper (R-branch) side of the band, and of the type

$$J'_{[(J' - n)/(J' - n + 1)], n} \leftarrow J_{[(J - n + 2)/(J - n + 1)], (n - 1)}$$

on the lower, P-branch side of the band origin. Within each series n is constant while $J' = J$ increases. These Q-branch series may contain up to 20 detectable transitions, initially close together and then spreading out in wavenumbers with the result that the strong high- J members of one such series overlap the weak members at the start of the next series. Some 15 cm^{-1} away from the band origin these Q-branch transitions fade out with the highest values for J and for $n = K'_c$.

The Q-branch transitions with high J -values and the lowest values of $n = K'_c$ ($n = 0, 1, 2, \dots$) form the intense Q-branch peak of the A-type band.

The B-type Band ν_5

The P- and R-branch structure of this band is qualitatively similar to the A-type band. However, with increasing doubly degenerate K_a -values individual transitions within the $|\Delta J| = 1$ clusters now decrease in wavenumber. On account of the b -type selection rule the clusters are now of the type

$$\begin{aligned}\bar{J}'_{[0/1], \bar{J}'} &\leftarrow J^*_{[1/0], J^*}, \\ (\bar{J}' - 1)_{[1/2], (\bar{J}' - 2)} &\leftarrow (J^* - 1)_{[2/1], (J^* - 2)}, \\ (\bar{J}' - 2)_{[2/3], (J' - 4)} &\leftarrow (J^* - 2)_{[3/2], (J^* - 4)}, \text{ etc.,}\end{aligned}$$

where $J^* = \bar{J}' + 1$ for P-branch and $J^* = \bar{J}' - 1$ for R-branch transitions. \bar{J}' is again the highest principal quantum number within each such cluster and has been inserted in the high-resolution traces of Figure 2. – The spreading out of the increasing number of transitions within each cluster and the eventual merging of successive clusters occurs this time at higher \bar{J}' -values than for the A-type band of Fig. 1 at $\bar{J}' \sim 45$ (see bottom left and right hand traces of Figure 2).

Q-branch transitions, which are now of the (doubly generate) type

$$J'_{[(J' - n)/(J' - n + 1)], n} \leftarrow J_{[(J - n + 1)/(J - n + 2)], (n - 1)}$$

below the band origin (P-branch side), and of the type

$$J'_{[(J' - n)/(J' - n + 1)], n} \leftarrow J_{[(J - n - 1)/(J - n)], (n + 1)}$$

above the band origin (R-branch side), form again series in which $n = K'_c$ is constant while $J' = J$ increases. As can be seen from a comparison of Fig. 2 with Fig. 1, these Q-branch series are this time more prominent above the band origin, whereas they show up most below the origin in the A-type band of Figure 1. Within $\sim 15 \text{ cm}^{-1}$ from ν^0 these series of Q-branch transitions again fade out with high values of $J' = J$ and high $n = K'_c$ (low K'_a).

The most characteristic feature of this band is of course the absence of intense high- J Q-branch transitions near the band origin. Instead, there occur in this case near the origin low- J transitions with small values of $n = K'_c$, entailing relatively large values of $K'_a \simeq J$ and therefore the lifting of the K'_a -degeneracy. This further reduces the small intensity of those low- J Q-branch transitions. – As may be seen from Fig. 2

(band origin), the non-degenerate Q-branch transitions of such pairs as

$$J'_{(J'-n),n} \leftarrow J_{(J-n+1),(n-1)}$$

and

$$J'_{(J'-n+1),(n-1)} \leftarrow J_{(J-n),n}$$

below and above ν^0 , respectively, are displaced almost symmetrically to either side of the band origin up to $J' = J \sim 10$.

3. Wavenumber accuracy of the FT-IR Instrument

In the numerical fitting of IR band structures the question arises: What accuracy can be attached to the wavenumber values of individual transitions as generated by the peak-finding procedure after Fourier transformation of the interferogram? – A hint of an answer to this question arises from the calibration of the spectrometer against a substance (here: N_2O) with accurately known [3] wavenumbers of its IR transitions. This indicates that the peaks of the calibration substance can be reproduced to within $1 \times 10^{-4} \text{ cm}^{-1}$, provided these peaks are carefully selected. This therefore represents a lower limit of the uncertainty range of the instrument. For an arbitrary sample however, such a preselection of peaks is neither desirable nor possible at the outset, and a consideration of the signal/noise ratio of individual absorptions seems necessary for the precise assessment of the accuracy of all peak wavenumber values. But this is hardly feasible. In addition, the usually immense number of peaks in the IR bands of asymmetric rotor molecules with frequent ‘blending’ (overlap) of absorptions of different intensities on account of the Doppler width together with the finite resolution of the instrument, raises the uncertainty range of peaks towards the higher limit of $1 \times 10^{-3} \text{ cm}^{-1}$.

A possibility for the assessment of the experimental reliability of the IFS 120 HR instrument seems to arise, however, from the observed spectrum itself: While the majority of Q-branch transitions in the wavenumber gaps between successive P- or R-branch clusters can be fitted to $\sim 2 \times 10^{-4} \text{ cm}^{-1}$, there occur also cases where an individual member of a series deviates by $5 \times 10^{-4} \text{ cm}^{-1}$ or more from expectation without an obvious spectral explanation, such as the blending of known transitions. These inexplicable discrepancies turn out to be of the same magnitude as the differences between peak wavenumber values which occur occasionally when the results from successive runs over the same band at only slightly different

pressure (but with the same calibration factor for the instrument) are compared: While the vast majority of peak wavenumber values agree with their counterparts to within $\sim 3 \times 10^{-4} \text{ cm}^{-1}$, larger discrepancies are also encountered occasionally.

On the basis of these observations we have adopted a value of $5 \times 10^{-4} \text{ cm}^{-1}$ as the largest acceptable deviation of a correctly identified transition from its calculated wavenumber. This limit is in good agreement with previous estimates of the wavenumber accuracy of the instrument at Giessen and of a similar instrument (BOMEM DA 3.002) at Ottawa [6].

For the fit of the ν_{12} band of furazan the imposition of a limit of $5 \times 10^{-4} \text{ cm}^{-1}$ on the acceptable differences between calculated and observed peak wavenumbers entailed the elimination from the fit of 163 from a total of 3334 IR peaks, and in the case of the ν_5 band 122 transitions had to be discarded from a total of 2392 assigned IR lines. Both figures lead to the conclusion that $\sim 5\%$ of the seemingly interpretable wavenumber values do not accurately enough correspond with expectation.

It seems appropriate to add in this context that while the described procedure leads to a reduction of the number of fitted IR transitions, we could achieve a very slight increase of that number through the ‘artificial splitting’ of some observed peak wavenumbers. A justification for that ‘manipulation’ arises as follows: The resolution of the instrument of $\sim 2.5 \times 10^{-3} \text{ cm}^{-1}$ is incompatible with the imposition of the 5 times smaller limit of $5 \times 10^{-4} \text{ cm}^{-1}$ on the accuracy of peak wavenumber values in the case of ‘blending lines’ of comparable intensity. In that case, the instrument will give the central wavenumber of the blending doublet which, if calculation indicated a doublet separation in the range $10\text{--}25 \times 10^{-4} \text{ cm}^{-1}$, would result in the elimination from the fit of both blending transitions. In view of the accuracy of rotational parameters and hence of the calculated doublet separations we considered it justifiable in such cases to add and subtract half the calculated separation to the observed wavenumber in order to save both transitions in the fit. In the wavenumber listings such ‘split peaks’ are marked with a dot.

4. Molecular Constants and Band Origins

The Ground State of Furazan

Since two sets of experimental data had been obtained for both IR bands, the LSQ fitting of each band was carried out twice.

In the first fit, in which the IR data obtained with the 'short' absorption cell under a sample pressure of ~ 5 mbar were used and which contained 1200 assigned peak wavenumbers in the case of ν_{12} (1109 IR- and 91 MW-lines) and 1035 transitions in the case of ν_5 (946 IR- and 89 MW-lines), the G.S. rotational constants previously deduced by microwave techniques [2] alone were inserted as fixed parameters while the G.S. quartic distortion constants were determined along with the excited state parameters and the band origins. At the end of that procedure the parameters of each excited state were held fixed and all eight constants of the G.S. were re-determined from an LSQ fit of the IR transitions of each band in conjunction with the 94 MW transitions within the G.S. The latter were weighted 100 times higher than the IR wavenumbers which were all given the same weight. Ideally, this procedure should have resulted in two identical sets of G.S. parameters (one set from each band). Very small differences (\sim one σ -limit) in the two G.S. sets remained however and, as the number of lines being fitted for each mode was approximately equal, a new set of G.S. constants was arrived at by straight averaging.

This improved set of G.S. parameters was then used in the fit of the two IR bands as observed in the 'long' cell under the smaller pressure of ~ 0.5 mbar. As before, the fitting procedure was reversed at the end to determine the best set of G.S. parameters from the data on each IR band. The method outlined above was repeated twice to result in an optimised set of molecular constants for the G.S. – This set is presented in Table 1, where the rotational constants are given in both wavenumber and frequency units to facilitate their comparison with the previous microwave results (Table 2 of [2]). Frequency values for the distortion constants are omitted though since a different Hamiltonian has been used in the earlier work.

Table 1. Optimised molecular constants of the vibrational ground state of furazan.

Rotational constants (in cm^{-1} and MHz)		Quartic distortion constants (in 10^{-7} cm^{-1})	
A	0.348 814 617 (21) ^a	Δ_J	0.832 70 (18)
	10 457.1991 (6)	Δ_{JK}	−0.276 00 (59)
B	0.332 944 775 (19)	Δ_K	0.768 14 (60)
	9 681.6408 (6)	δ_J	0.332 47 (6)
C	0.167 572 473 (19)	δ_K	0.625 57 (27)
	5 023.6964 (6)		

^a Uncertainties are one σ -limit and given in units of the last quoted digit.

We intend to use the G.S. constants of Table 1 in the analysis of further vibrational bands of furazan.

The States $\nu_{12}=1$ and $\nu_5=1$
and the Band Origins

With the G.S. constants held fixed at their optimised values given in Table 1, the identified IR transitions to and the MW transitions within the two excited states were LSQ-fitted to extract the rotational parameters and the band origins ν_i^0 . The previously reported MW transitions of the excited states (Appendix of [2]) were given a weight of 100 in these fits since their frequency uncertainty is at least by that factor smaller than the adopted uncertainty limit of the IR measurements (less than 0.1 MHz compared with $15 \text{ MHz} \pm 5 \times 10^{-4} \text{ cm}^{-1}$). From a total of 3262 peak wavenumber values in the case of ν_{12} and from 2359 data for the ν_5 -band the parameters collected in Table 2 were obtained. Comparison with Table 1 shows that the molecular constants of the two excited states emerge with uncertainties comparable with those of their counterparts in the G.S., and the band origins ν_i^0 indicate an internal consistency (σ) of better than $1 \times 10^{-6} \text{ cm}^{-1}$ for both states. – As would be expected for a molecule of mass 72 a.m.u. with a comparatively rigid ring structure (lowest fundamental at $\sim 631 \text{ cm}^{-1}$), neither the previously observed MW spectra nor the fits of the two IR bands revealed any systematic deviations which could have indicated the relevance of sextic distortion constants. Accordingly, these constants were taken as zero for the two excited states and the G.S. alike.

The top of Table 2 contains general information on the two bands and statistical information on the fits. To facilitate the comparison with previous MW data, the rotational constants are again given in wavenumber and frequency units. The standard deviations of these fits are not drastically larger than the deviations of measured peak wavenumbers of the calibration substance from literature values [3] and we feel on that ground that the two vibrational origins of furazan may be quoted with an absolute uncertainty of 0.0001 cm^{-1} .

5. Appraisal of Results

The success of the present analyses indicates that the fundamental modes $\nu_{12}=1$ and $\nu_5=1$ of furazan, although separated by only some 50 cm^{-1} , interact with each other and with other modes of vibration so little as to make the manifestations of such vibrational

Table 2. Molecular constants and band origins for the fundamental vibrations ν_{12} and ν_5 of furazan.

Mode, Level	$\nu_{12}=1$	$\nu_5=1$
C_{2v} symmetry species	B_1	A_1
Selection rule/type	μ_a/A -type	μ_b/B -type

Diagrammatic description

Fitted transitions		
$N_{P\text{-branch}}$	975	742
$N_{Q\text{-branch}}$	1218	823
$N_{R\text{-branch}}$	978	705
$N(\text{IR})_{\text{total}}$	3171	2270
Standard deviation of IR fit	$2.0 \text{ E}-4 \text{ cm}^{-1}$	$1.9 \text{ E}-4 \text{ cm}^{-1}$
<hr/>		
MW transitions	91	89
$N(\text{IR} + \text{MW})_{\text{total}}$	3262	2359
Standard deviation (IR + MW)	$1.2 \text{ E}-5 \text{ cm}^{-1}$	$1.0 \text{ E}-5 \text{ cm}^{-1}$
<hr/>		
Rotational constants (in cm^{-1} and MHz) ^a		
A	0.349 291 597(19) ^b 10 471.4986 (6)	0.349 088 718(25) 10 465.4165 (8)
B	0.323 097 359(18) 9 686.2151 (6)	0.322 523 812(22) 9 669.0206 (7)
C	0.167 154 078(21) 5 011.1532 (6)	0.167 695 680(23) 5 027.3900 (6)
<hr/>		
Quartic distortion constants (in 10^{-7} cm^{-1})		
Δ_J	0.830 12(12)	0.850 47 (17)
Δ_{JK}	-0.231 41(65)	-0.329 10 (79)
Δ_K	0.780 86(65)	0.836 36(136)
δ_J	0.337 60 (6)	0.318 38 (9)
δ_K	0.660 22(25)	0.666 83 (34)
<hr/>		
Band origin ν^0	952.612 271(1)	1005.353 563(1)

^a Conversion factor $c = 29\,979.2458 \text{ E} + 6 \text{ cm/sec}$.^b Uncertainties are one σ -limit and given in units of the last quoted digit.

resonances too small for observation by current techniques. Both bands therefore satisfy the assumption underlying the Gambi computer package [4] that the rotational levels of the states $\nu_{12}=1$ and $\nu_5=1$ can be calculated accurately enough from the Hamiltonian of Watson [5]. A similar situation has been verified in the meanwhile for two further fundamentals of furazan,

while the occurrence of vibrational resonances in the fundamentals below 900 cm^{-1} has been detected in the previous study by DRM microwave techniques [2].

Under the described circumstances, the quality of the here deduced molecular constants, as given in Tables 1 and 2, is characterised by the correlation matrices of the LSQ fits of the data. For this reason, these matrices are reproduced below.

IV. Discussion

The present study brings to fruition research in molecular spectroscopy by three different experimental techniques, namely DRM microwave spectroscopy [7] to begin with [2], LMDR experiments [8, 1] as the link between rotational and vibrational spectroscopy and, finally, high-resolution FT-IR spectroscopy. This begs for an appraisal of the contribution by each technique to the whole and to the other two.

The analysis of a highly-resolved IR band commonly requires that not only the band origin ν^0 , but also the molecular constants of the two states interconnected by that band be determined. For an asymmetric rotor this demands the determination of $2 \times (3+5)+1=17$ parameters if sextic distortion constants are assumed or known to be insignificant (as in the present case). Since the chances of a researcher's correct interpretation (assignment) of a sufficiently large number of observed rovibrational transitions either by experience or by intuition are remote, computer routines have been devised (e.g. [4]) which allow the modelling of an IR band structure as a function of assumed trial parameters. Once sufficient similarity of such a model with the observed band structure is achieved, the six rotational constants and the band origin, and then the 10 (or more) distortion constants may be successively deduced on the basis of more and more correctly identified rovibrational transitions.

This difficult, and certainly tiresome, task can be halved if at least the molecular constants of the ground vibrational state are known beforehand from pure rotational, usually Stark effect modulation, microwave (MW) spectroscopy. In the present case of furazan, the good sensitivity and extreme molecular selectivity of DRM MW techniques was taken advantage of to yield not only the G.S. parameters – as usual – but also the rotational constants of the excited states, although these all lie above 600 cm^{-1} . As a

1. Correlation matrices of the LSQ fits for the determination of the molecular constants of Table 1 from 94 MW-transitions in the G.S. in conjunction with 3171 rovibrational transitions of the A-type band ν_{12} (right triangle) and in conjunction with 2270 transitions of the B-type band ν_5 (left triangle).

1.0000	−0.2928	−0.3114	0.4150	−0.2100	0.5830	0.1645	0.3084
−0.1367	1.0000	0.6803	−0.1838	0.1200	−0.0759	0.1101	0.0132
−0.3097	0.6745	1.0000	−0.7312	0.5719	0.1450	0.5461	0.0294
0.0780	−0.1444	0.4069	1.0000	−0.9256	−0.0614	−0.5117	0.3586
0.3684	0.0418	−0.0816	−0.7786	1.0000	0.1266	0.4551	−0.4421
0.4688	0.0870	0.3217	−0.0483	−0.0216	1.0000	0.7494	0.1203
−0.0780	0.2763	0.7445	−0.1989	−0.2285	0.7191	1.0000	−0.1769
−0.0413	0.1031	0.3851	0.3786	−0.5884	0.2367	0.3051	1.0000

2. Correlation matrix of the LSQ determination of the molecular constants of the state $\nu_{12}=1$, as given in Table 2.

1.0000								
−0.3613	1.0000							
−0.3593	0.6641	1.0000						
0.4341	−0.1944	−0.7617	1.0000					
−0.2445	0.1258	0.6191	−0.9360	1.0000				
0.6300	−0.1756	0.0847	−0.0323	0.1058	1.0000			
0.1902	0.0419	0.5374	−0.5309	0.4929	0.7451	1.0000		
0.3428	−0.0184	−0.0670	0.4279	−0.4941	0.1400	−0.2022	1.0000	
0.0252	−0.1716	−0.0623	−0.0019	0.0040	0.0426	0.0283	−0.0007	1.0000

3. Correlation matrix of the LSQ determination of the molecular constants of the state $\nu_5=1$, as given in Table 2.

1.0000								
−0.2159	1.0000							
−0.3193	0.6618	1.0000						
0.1742	−0.1724	−0.4933	1.0000					
0.2634	0.0789	0.0228	−0.7795	1.0000				
0.5584	−0.0590	0.2364	−0.0265	−0.0082	1.0000			
0.0256	0.1734	0.6904	−0.2621	−0.1342	0.7319	1.0000		
0.0808	0.0468	0.2745	0.4011	−0.5629	0.2395	0.2213	1.0000	
0.0197	−0.1553	−0.0488	0.0008	−0.0068	0.0444	0.0269	0.0067	1.0000

The sequence of variables in all four LSQ fits was as follows: $A-B$, B , A_J , A_{JK} , A_K , $B-C$, δ_J , δ_K , ν^0 .

result, the entire IR band structure could be pre-calculated on the basis of those DRM MW results [2]. The otherwise quite enormous task of the IR spectroscopist was thus effectively reduced to the determination of one single parameter, namely the band origin ν^0 . A good value for this parameter had been deduced, however, on the basis of the same DRM MW work from the LMDR experiments [1]. Consequently, the gradual and presumably slow approach towards the correct values of the 17 molecular constants could be completely and confidently by-passed, and the utterly simple analysis of the IR bands could be used to see whether an improvement of the results from the first two techniques was possible through the addition of data from FT-IR spectroscopy. – We feel that the answer to this question has to be affirmative:

The enormous amount of data from FT-IR certainly allows an improvement of the distortion constants derived by MW spectroscopy. In the pure rotational spectrum of furazan between 12–40 GHz (0.4–1.3 cm^{−1}) P-branch transitions are completely absent and observable R-branch transitions are below 15 in number and restricted to very low values of J . The FT-IR bands, in contrast, exhibit between 700 and 1000 transitions of either type with J -values up to 50, and the number of Q-branch transitions in the IR spectrum is about 10 times higher than in the MW spectrum, extending to J -values twice as high as in the latter. Hence, the distortion constants derived from the IR fits must be considered superior to their counterparts from MW fits on account of the considerably larger number of data and the larger J -range of the

fitted IR transitions. Together, these two features outweigh the smaller accuracy than in MW work of individual IR data (peak positions).

The contribution of the MW data to the results deducible from the IR bands alone cannot be disregarded either. It stems from the 100 times superior precision of MW frequencies over IR measurements, and reduces the statistical uncertainties associated with the IR results alone. The test shows that the inclusion of the MW transitions in the LSQ fits of the IR bands reduces the uncertainties of the rotational constants by factors between 3 and 5 and those of the distortions constants by a factor of at least 2. In combination, the mutual contributions from FT-IR to MW results and from MW data to IR results lead to a reduction of the previous error limits [2] on the MW rotational constants by a factor of 10, and the consistency of the v^0 -values is raised over the LMDR results [1] by a factor of at least 100, though this has to be reduced in absolute terms to about 20 on account of uncertainties in the IR calibration. The reduction, on the other hand, of the standard deviations of the fits by a factor 20 (Table 2) through the inclusion of the MW transitions should perhaps be taken as a 'statistical artifact' resulting from the 100 times larger weight of the relatively few MW lines.

In summary, the present work seems to lead to the following conclusions: Firstly, the prior study of excited states by DRM microwave eliminates the chores otherwise encountered in the analysis of high-resolution IR bands. Secondly: On account of considerably

larger numbers of transitions over a wider range of J -values, FT-IR bands yield distortion constants superior to those from microwave spectroscopy. Thirdly: The precision of additional MW transitions helps towards a more precise determination of the rotational constants of a molecule than is possible from current IR techniques alone.

Acknowledgements

The author gratefully acknowledges financial support for this project from the Royal Society through their German sister organisation, the Deutsche Forschungsgemeinschaft. He was able to obtain this support through the help of Professor D. H. Whiffen, F.R.S. (formerly: Newcastle upon Tyne) to whom he feels deeply indebted. He also wishes to thank all members of the spectroscopy group at Giessen for their conviviality, and he would like to thank particularly Dipl.-Ing. Klaus Lattner of the very diligent and competent operation of the Bruker IFS 120 HR instrument. The goodwill and the hospitality of Professor Manfred Winnewisser and Dr. Brenda P. Winnewisser, which has made this present study possible, is most deeply appreciated.

It is a pleasure to thank Dr. Brenda P. Winnewisser and Professor A. Ruoff for their critical reading of the draft or manuscript of this paper and for their valuable suggestions for improvement.

- [1] O. L. Stiefvater, *Z. Naturforsch.* **46a**, 599 (1991).
- [2] O. L. Stiefvater, *Z. Naturforsch.* **45a**, 1117 (1990).
- [3] G. Guelachvili and K. N. Rao, 'Handbook of Infrared Standards', Academic Press, London 1986.
- [4] A. Gambi, M. Winnewisser, and J. J. Christiansen, *J. Mol. Spectroscopy* **98**, 413 (1983).
- [5] J. K. G. Watson, in: *Vibrational Spectra and Structure*. J. R. Durig, Editor, Vol. 6, Elsevier, Amsterdam 1977.
- [6] G. Moruzzi, P. Riminucci, F. Strumia, B. Carli, M. Carlotti, R. M. Lees, I. Mukhopadhyay, J. W. C. Johns, B. P. Winnewisser, and M. Winnewisser, *J. Mol. Spectroscopy* **144**, 139 (1990).
- [7] O. L. Stiefvater, *Z. Naturforsch.* **30a**, 1742, 1756 (1975).
- [8] H. Jones, in: *Modern Aspects of Microwave Spectroscopy*. G. W. Chantry, Editor, Academic Press, London 1979.